GEOCHRONOLOGY

Open Access

EGU

Technical Note: Noble gas extraction procedure and performance of the Cologne Helix MC Plus multi-collector noble gas mass spectrometer for cosmogenic neon isotope analysis

Benedikt Ritter, Andreas Vogt, and Tibor J. Dunai

Institute of Geology and Mineralogy, University of Cologne, Zülpicher Straße 49b, Köln 50674, Germany

Correspondence: Benedikt Ritter (benedikt.ritter@uni-koeln.de) and Tibor J. Dunai (tdunai@uni-koeln.de)

Abstract. We established a new laboratory for noble gas mass spectrometry that is dedicated to the development and application to cosmogenic nuclides at the University of Cologne (Germany). At the core of the laboratory are a state-of-the-art high-mass-resolution multicollector Helix MC Plus (Thermo Fisher Scientific) noble gas mass spectrometer and a novel custom-designed automated extraction line. The mass spectrometer is equipped with five combined Faraday multiplier collectors, with 10^{12} and $10^{13}\,\Omega$ preamplifiers for faraday collectors. We describe the extraction line and the automated procedure for cosmogenic neon and the current performance of the experimental set-up. Performance tests were conducted using gas of atmospheric isotopic composition (our primary standard gas), as well as CREU-1 intercomparison material, containing a mixture of neon of atmospheric and cosmogenic composition. We use the results from repeated analysis of CREU-1 to assess the performance of the current experimental set-up at Cologne. The precision in determining the abundance of cosmogenic ^{21}Ne is equal to or better than those reported for other laboratories. The absolute value we obtain for the concentration of cosmogenic ^{21}Ne in CREU is indistinguishable from the published value.

1 Introduction

Cosmogenic Ne isotopes are stable and compared to other cosmogenic radionuclides (e.g. ^{10}Be, ^{26}Al) exhibit the potential to date beyond the physical limit of radionuclides. The particular strength of cosmogenic neon is its application to date quartz clasts of very old surfaces (> 4 Ma) or very slowly eroding landscapes (< 10 cm Ma^{-1}), which is unattainable with most other radionuclides (Dunai, 2010). Cosmogenic Ne analysis can be applied to a range of neon-retentive minerals (e.g. quartz, olivine and pyroxene), amongst which quartz is the most commonly used. Ne can be measured on conventional sector field noble gas mass spectrometers, is less time consuming and requires less sample-preparation compared to AMS measurements required for the cosmogenic radionuclides. Recent studies used cosmogenic Ne for dating old surfaces (e.g. Ritter et al., 2018; Dunai et al., 2005; Binnie et al., 2020), reconstructing erosion rates (e.g. Ma et al., 2016) or ^{10}Be / ^{21}Ne burial dating (e.g. McPhillips et al., 2016). The advantage of also using other minerals than quartz led to several studies using ^{21}Ne to date for example basalt flows (e.g. Espanon et al., 2014; Gillen et al., 2010). Neon has three stable isotopes ^{20}Ne, ^{21}Ne and ^{22}Ne, of which ^{20}Ne is the most abundant; the atmospheric ^{21}Ne / ^{20}Ne and ^{22}Ne / ^{20}Ne ratios are 0.002959 ± 0.000022 and 0.1020 ± 0.0008, respectively (Eberhardt et al., 1965). There are several recent redeterminations of the atmospheric ^{21}Ne / ^{20}Ne ratio (e.g. Honda et al., 2015; Wielandt and Storey, 2019; Saxton, 2020; Györe et al., 2019) one of which yields a $\sim 2\%$ lower value (Honda et al., 2015). For the evaluation of our data, we utilise the ^{21}Ne / ^{20}Ne value of Wielandt and Storey (2019) of 0.0029577 ± 0.0000014 and for ^{22}Ne / ^{20}Ne that of Eberhardt et al. (1965). Note that in the context of the determination of the *abundance* of cosmogenic nuclides in a sample, eventual differences between the used and the actual value of the atmospheric ^{21}Ne / ^{20}Ne ratio are unimportant, if (i) atmospheric neon is used as calibration gas, (ii) the same value for the composition of atmospheric neon is used consistently

throughout the evaluation of the isotope data (mass discrimination etc.) and calculation of abundances, and (iii) the atmospheric value used is reported along with the data.

All three neon isotopes are produced in about equal proportions by neutron spallation in quartz (Niedermann et al., 1994). Due to the lower abundances of ^{21}Ne and ^{22}Ne as compared to ^{20}Ne in air, and the ubiquitous presence of atmospheric neon in samples, any contribution from cosmogenic production in samples is most easily picked up with the former two isotopes. Consequently, the neon three-isotope diagram with ^{20}Ne as common denominator (Niedermann et al., 1994; Niedermann, 2002) is customarily used to assess ^{21}Ne data for the presence of terrestrial cosmogenic Ne and its discrimination from other non-atmospheric Ne components (Dunai, 2010). The latter may be nucleonic Ne and/or mantle-derived Ne. Hence, the accurate determination of cosmogenic Ne and its discrimination from other components requires the accurate discrimination from any other component.

Common isobaric interferences for neon measurements are at $m/e = 20$ (^{40}Ar^{2+}, H^{19}F$^+$ and H$_2^{18}$O$^+$ interfering with ^{20}Ne$^+$), at $m/e = 21$ (^{20}NeH$^+$, interfering with ^{21}Ne$^+$) and at $m/e = 22$ (^{44}CO$_2^{2+}$ interfering with ^{22}Ne$^+$). ^{40}Ar^{2+} and ^{12}C^{16}O$_2^{2+}$ interferences are considered to be the main challenges for neon analysis. Recent studies demonstrated the ability of the Helix MC Plus to fully resolve the ^{40}Ar^{2+}, H^{19}F$^+$ and H$_2^{18}$O$^+$ peaks from the ^{20}Ne$^+$ peak (e.g. Honda et al., 2015; Wielandt and Storey, 2019) and its ability to reliably measure ^{21}Ne at an off-centre peak position that is free of interference from ^{20}NeH$^+$ (Honda et al., 2015; Wielandt and Storey, 2019). The remaining interference of ^{12}C^{16}O$_2^{2+}$ at $m/e = 22$ can be corrected via monitoring of the ratio of double- to single-charged CO$_2$ in between samples (Honda et al., 2015) or the measurement of ^{13}C^{16}O$_2^{2+}$ at $m/e = 22.5$ during sample analysis (Wielandt and Storey, 2019). Recently mass spectrometers with higher resolution have become available, which permit almost full separation of ^{12}C^{16}O$_2^{2+}$ and ^{22}Ne (Farley et al., 2020).

Besides the resolution and characteristics of a noble gas mass spectrometer to resolve and quantitatively determine neon compositions of an unknown sample, the calibration, sample extraction and purification are crucial to achieving accurate and reproducible results. Automation of extraction protocols and workflows may assist in achieving a high degree of reproducibility by eliminating inaccuracies or errors by operators having a variable degree of expertise. In this paper, we describe the current set-up of the noble gas mass spectrometer and its automated extraction line that is located in the Institute of Geology and Mineralogy at the University of Cologne (Germany), and we review its performance for neon analysis.

2 Experimental set-up

2.1 Noble gas mass spectrometer

The Cologne noble gas laboratory is equipped with a Helix MC Plus from Thermo Fisher Scientific with five CFM (combined Faraday multiplier) modules, called "Aura". The central, axial module (Ax) is fixed in position, and the four remaining modules (L1, L2 on the low mass side, and H1, H2 on the high mass side of Ax) can be moved. The mass spectrometer configuration and performance is mostly equivalent to those described elsewhere (Honda et al., 2015; Wielandt and Storey, 2019); here we describe potential differences in configuration and performance parameters that may be unique to a given instrument (Fig. 1).

In the instrument at Cologne University, all but one of the Faraday amplifiers are equipped with 10^{13} Ω resistors, one with 10^{12} Ω (H2). The L1 module has 0.3 mm wide collector slits, and all other modules have 0.6 mm wide slits. The CFM at L1 configuration is flipped (i.e. the relative positions of the Faraday and multiplier are swapped) as compared to the standard configuration, which is the only difference from the standard configuration. The two SAES NP10 getters, at the source and the multiplier block, are kept at room temperature during analysis.

For neon isotope analysis of calibrations and samples, we utilise the H1, Ax and L1 CFMs (^{20}Ne$^+$ L1 Faraday; ^{22}Ne$^+$ H1 Faraday; ^{21}Ne$^+$ L1 multiplier; CO$_2^+$ H1 Faraday; for blanks we utilise the L1 multiplier also for ^{20}Ne$^+$ and ^{22}Ne^{++}). With the widest source slit (0.25 mm), mass resolution (at 5 % peak valley) and mass resolving power (between 10 % and 90 % of peak) on the L1 detector with 0.3 mm collector slit width are approximately 1700 and 6500, respectively. For the Ax and H1 detectors with 0.6 mm collector slit, the corresponding values are approximately 1000 and 6000, respectively. As such the system allows the interference-free determination of ^{20}Ne and ^{21}Ne; for ^{21}Ne this entails measuring at an off-centre peak position (Honda et al., 2015; Wielandt and Storey, 2019).

2.2 Extraction line

The Cologne noble gas extraction and purification line has a modular design (Fig. 1). Modules are (i) extraction (currently only laser extraction; to be joined by a crushing device), (ii) calibration gas pipettes and volumes, (iii) clean-up, and (iv) cryogenic separation. The calibration module is physically linked to the clean-up module, and the other modules can be separated, if required. Among the common features of all modules is that all valves and tubing in contact with the sample gas are made of metal; tubing is of stainless steel or vacuum-annealed copper. Furthermore, all valves used for handling of sample and calibration gas are pneumatically actuated all-metal diaphragm valves (Fujikin MEGA-M LA; FWB(R)-71-6.35) that can be operated at
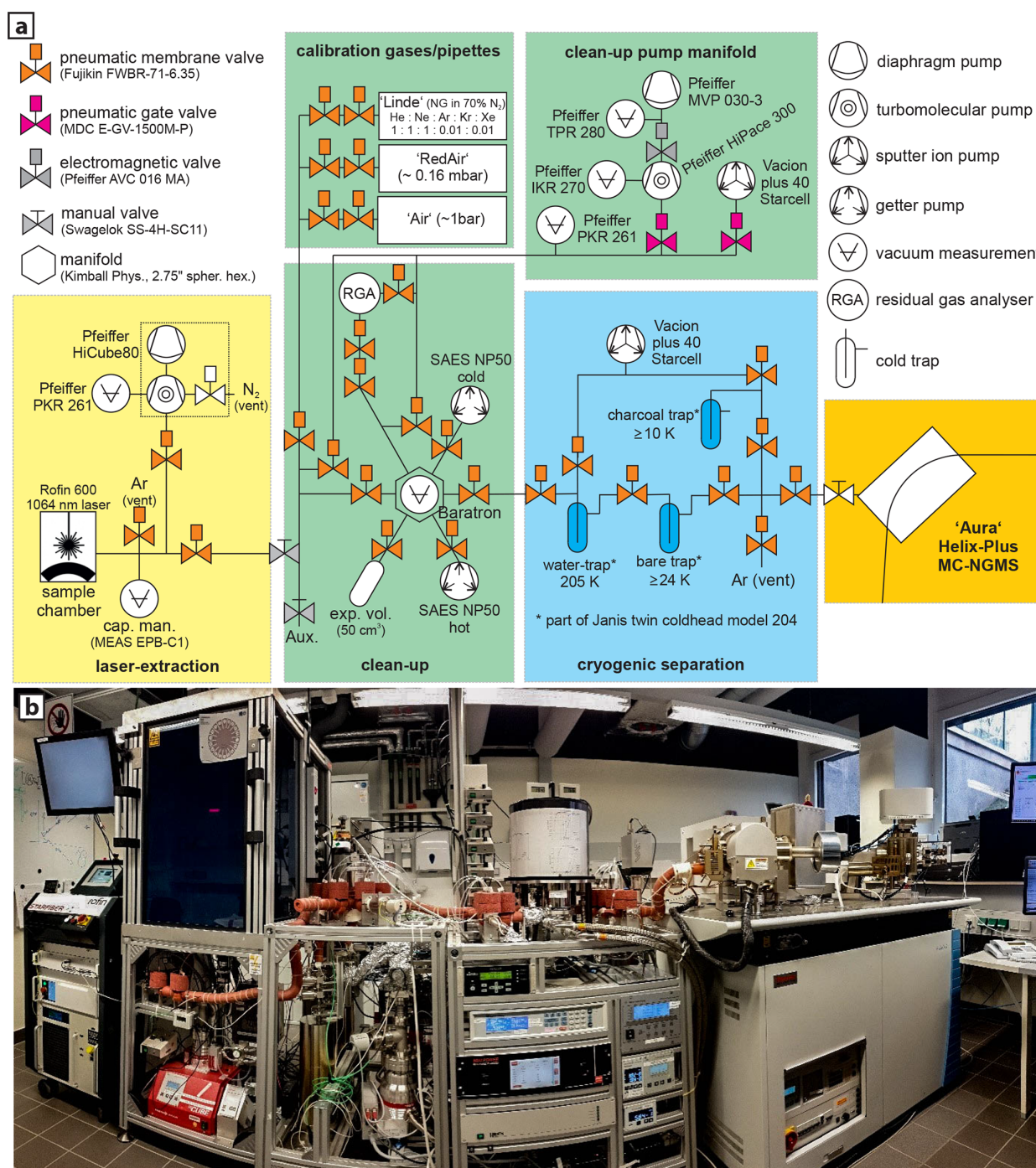
Figure 1. (a) Schematic plan and **(b)** picture of the noble gas extraction and purification line at the University of Cologne. From left to right: Rofin Starfiber 600, full-protection laser cage (laser protection windows P1P10, Laservision) housing the laser extraction, clean-up unit, cryogenic separation unit and the Helix Plus NG-MCMS "Aura". The laboratory is temperature-stabilised to $\pm 0.5\,°C$. Further description is provided in the text.

high temperature (up to $350\,°C$). Tubing and valves in contact with sample gas are continuously kept at constant temperature between 160 and $200\,°C$; exceptions are the functional traps and portions of the tubing in the cryogenic separation. Temperature is maintained with heating tapes (Horst HS $450\,°C$) and is controlled section-wise (Horst HT30). The temperature of the heated sections is controlled to $\pm 1\,°C$. Thermal insulation is achieved with high-temperature resistant silicone foam (HOKOSIL®; resists $\leq 280\,°C$; permitting bake-out at higher than operation temperatures). Vac-

uum connections used are VCR (for Fujikin valves), CF (for adapters, getters and manifold in clean-up) and Swagelok (for flexible tubing between modules and between ports of the cryogenic separator (Swagelok 321 Stainless Steel Flexible Tubing with XBA adapter; copper tubing). Tubing and valves are 1/4 in. outer diameter (Swagelok) or equivalent (VCR, Fujikin)). The overall internal volume of the extraction line (laser extraction, clean-up and cryogenic separation) is 530 cm^3. Outside the volume used for sample preparation, CF connections are used throughout. A schematic overview and picture of the extraction line is provided in Fig. 1.

More specific information about the individual modules is given in the following:

i. *Laser extraction module (Fig. 1).* Up to 18 tungsten cups are loaded in a sample revolver housed in a DN 200 CF flange sandwich. The sample revolver is machined from molybdenum, which permits the heating of the tungsten cups while being situated in the revolver. To minimise heat loss through conduction, the cups sit on shards of zirconia (synthetic, cubic-stabilised ZrO_2). The tungsten cups can hold up to ~600 mg quartz. The tungsten cups are reused. When analysing quartz, tungsten cups are emptied with a suction micropicker (Micropicker MPC100; VU Amsterdam), while remaining in the sample revolver. In cases where samples are melted during extraction, tungsten cups could be cleaned in HF (then of course outside the revolver). For sample loading the volume containing the revolver is vented and continuously flushed with high-purity nitrogen. During laser extraction the pressure is monitored (MEAS EPB-C1 sensor, welded into a male VCR connector; Disynet), and in case of an eventual failure of the viewport, the extraction volume is automatically purged with Argon. Energy for the heat extraction is provided by an output-tuneable 600 W fibre laser (Rofin StarFiber600) at 1064 nm wavelength through galvanometer scanner optics (Rofin RS S 14 163/67 0°) and a sapphire viewport (Kurt Lesker, VPZL-275DUS). For neon extraction of quartz, the cups are covered with tungsten lids; the heating occurs via scanning of the lids (scanning speed 20 cm s^{-1}; rastering a circular area of 10 mm diameter) with a defocussed (~0.5 mm diameter) continuous wave beam with 100 W power for 15 min. Copper (melting point 1085 °C), placed in the cup assemblies, melts at 80 W laser power (15 min extraction time); we assume that at 100 W laser power the internal temperature is ≥1200 °C. The temperature of the top of the tungsten lids is monitored with a pyrometer (CellaTemp PA 29 AF 2/L; Keller HCW). The laser extraction has a dedicated pumping unit (Pfeiffer HiCube80). Pressures attained after sample loading and heating of the revolver (via short-term laser heating – stepwise increased to 200 W – of an empty tungsten cup; the external housing flanges reach ~50 °C during this treatment; tem-

peratures in adjacent cups in the revolver stay below 156.6 °C, which was verified with Indium wire) are usually <5 × 10^{-9} mbar (the lower limit of the pressure gauge used) after one night of pumping. Typical blanks, obtained via heating of an empty tungsten cup assembly, are ~0.3 fmol neon. A detailed description of this novel laser furnace will be provided elsewhere.

ii. *Calibration gas pipette module (Fig. 1).* The gas pipettes are assemblies of male and female versions of pneumatically actuated Fujikin diaphragm valves (MEGA-M LA; FWB(R)-71-6.35); the reservoirs were manufactured by Caburn-MDC, and the insides of the reservoirs are electropolished. We currently have three different gases available for noble gas calibration ("Linde", "Air", "RedAir"). "Linde" is a noble gas mixture in nitrogen (9.889 ± 0.009 % He, 10.00 ± 0.01 % Ne, 10.01 ± 0.01 % Ar, 0.00987 ± 0.0003 % Kr; 0.01023 ± 0.00002 % Xe; all uncertainties are ±2σ; remainder N$_2$; prepared gravimetrically by Linde; values as certified by Linde according to DIN ISO 6141) the He is enriched in ^{3}He (12.3 ± 0.3 R$_a$; ±2σ; value as certified by Linde according to DIN ISO 6141), and the remaining noble gases have atmospheric composition. We assume that the cryogenically purified atmospheric gases used by Linde were not fractionated during this process; we have verified this for Ne within the limits of uncertainties reported in this paper. "Air" is a reservoir of air at atmospheric pressure and "RedAir" a reservoir of air at reduced pressure (lab name RedAir is the abbreviation of that fact). For the neon determinations we utilise RedAir. The volumes of all reservoirs and the pipettes have been determined relative to a gravimetrically calibrated gas volume (an assembly of a Swagelok SS-4H valve and a Swagelok SS-4CS-TW-50 miniature cylinder; repeatedly weighed (Sartorius MSA524P-1000-DI; the balance was calibrated prior to calibration of the reference volume) under vacuum and filled with air at a temperature (n = 16), pressure and relative humidity measured with traceable and/or certified sensors (thermometer: testo 110; manometer: Greisinger GMH 3181-12, DKD certificate D19853, D-K-15070-01-01; hygrometer: VWR traceable 628-0031); reference volume is 51.37 ± 0.18 cm^3 (±1σ)). All other volumes (piping of the calibration gas filling line; pipettes and reservoirs) were determined by taking pressure readings (MKS Baratron, Type 628FU5TCF1B) from repeated step-wise expansion of gases. The temperature in the room where these calibrations were conducted was stable to ±0.5 °C over the course of the calibrations. The thus determined volumes of the reservoir and pipette of RedAir are 8740 ± 35 and 1.457 ± 0.006 cm^3 (±1σ), respectively. For filling of the RedAir reservoir one pipette volume of air was expanded into the reservoir;

the temperature, pressure and humidity at the time of filling of the pipette were measured with a traceable and certified sensor (same as above). The first pipette volume extracted from the RedAir reservoir contained $4.020 \pm 0.027 \times 10^{-9} \, cm^3$ ($\pm 1\sigma$) atmospheric neon at standard temperature and pressure ($179 \pm 1 \, fmol$ atmospheric neon; $\pm 1\sigma$).

iii. *Clean-up module (lab name "Sputnik" referring to the shape and protrusions of the central manifold and its faint resemblance to the first satellite; Fig. 1).* Arranged around a central hexagonal 8-port manifold (Kimball Physics, 2.75″ spherical hexagon) are the sample/calibration inlet, the pumping outlet, a pipette leading to a residual gas analyser (Hiden HAL/3F PIC), two SAES NP50 getters (one operated hot; heating current 1.6 A; ~ 300 °C, the other at room temperature; getters are housed in SAES GP 50 W2F bodies; water cooling is optional, not used during sample analysis), an optional expansion volume, an internally heated capacitance manometer (MKS Baratron, Type 628FU5TCF1B; @ 100 °C) and the outlet to the cryogenic separation unit (Fig. 1). The sample/calibration inlet tubing has an auxiliary port, which for example is used for the crushing extraction module (build around a T4S crushing unit, VU Amsterdam). The clean-up module is pumped via a manifold connected through gate valves (MDC E-GV-1500M-P) to a turbopump (Pfeiffer HiPace 300; backed by a membrane pump, Pfeiffer MVP 030-3) and an ion pump (Agilent, Vacion 40 plus Starcell).

iv. *Cryogenic separation module (Fig. 1).* The centre of this module is a double-cold trap unit (Janis, twin cold-head model 204) that has inlet and outlet lines to three traps: a water trap (operated at 205 K), a bare steel trap ($\geq 24 \, K$) and a charcoal trap ($\geq 10 \, K$). The cold trap unit is controlled by a Lakeshore 336 Controller (Cryotronics). This module is pumped by an ion pump (Agilent, Vacion 40 plus Starcell).

The performance of the bare cold trap unit for He, Ne and Ar separation was calibrated using the Residual Gas Analyser (Hiden HAL/3F PIC). Neon is quantitatively adsorbed on the bare trap at 24 K ($> 99.9985 \, \%$ is adsorbed at 24 K; Fig. 2); in equilibrium about 60 % of the helium is adsorbed at 24 K. We use this to separate helium from neon. Helium is removed (distilled off in disequilibrium) either to the ion pump or the 10 K charcoal head, the latter if the He is to be retained for analysis. Neon is fully released from the bare trap at 80 K; at this temperature argon is quantitatively retained on the bare trap, permitting quantitative separation of the two gases (Fig. 2).

Besides its functionality to separate noble gases from each other the bare trap serves as cold trap during Ne analysis (held at 80 K) and replaces a liquid-nitrogen-cooled trap,
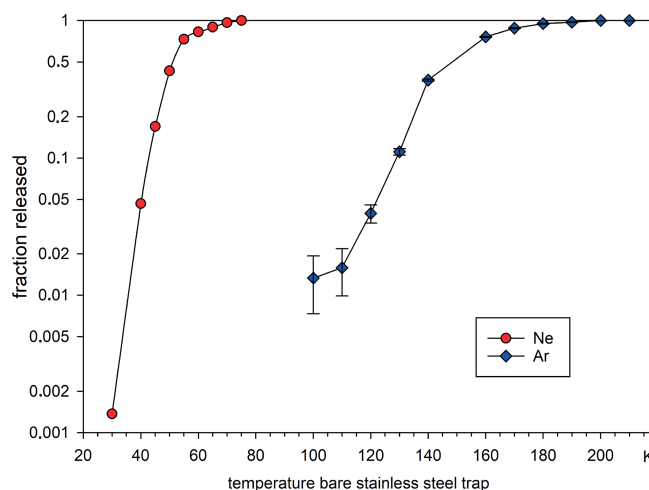

Figure 2. Desorption curves of Ne and Ar on the stainless-steel cold trap measured with the Hiden quadrupole. The uncertainties of the argon determinations at low fractions released are due to a significant Ar background of the quadrupole (e.g. measurement at 100 K was just 5 % higher than the background).

which would otherwise customarily be used for this purpose. The latter may introduce intensity fluctuations during analysis due to changing coolant level, which we avoid with our set-up. The last pneumatically actuated valve before the Helix-Plus MCMS serves as inlet valve, and the manual valve of the Helix-Plus MCMS is permanently open.

2.3   Automation

The extraction and purification line can either be operated manually, via a switchboard for the pneumatic valves and the components' original controllers, or automatically via LabView. Manual operation is mainly used for development of analytical routines, automatic operation generally for sample and calibration-gas analysis. Automatic operation liberates the operator from conducting necessarily repetitive tasks and thus helps to prevent mistakes and inconsistencies from oversight or negligence; it allows gas purification and separation to be conducted under precisely identical conditions. The latter is also assisted by avoiding liquid coolants, which commonly are affected by variable coolant levels (unless automatically filled with a suitably precise system or an experienced and conscientious operator). Currently the laser system is operated manually (due to safety regulations); all subsequent steps – until admission of the gas to the mass spectrometer – are automated utilising LabView (Version 2018) in a Windows 10 environment. The mass spectrometry analysis of the purified gas is conducted with Qtegra (Thermo Fisher Scientific).

Valve control electronics were developed and implemented in-house, including digital input/output modules (I/O modules from National Instruments) and RS-232 commu-
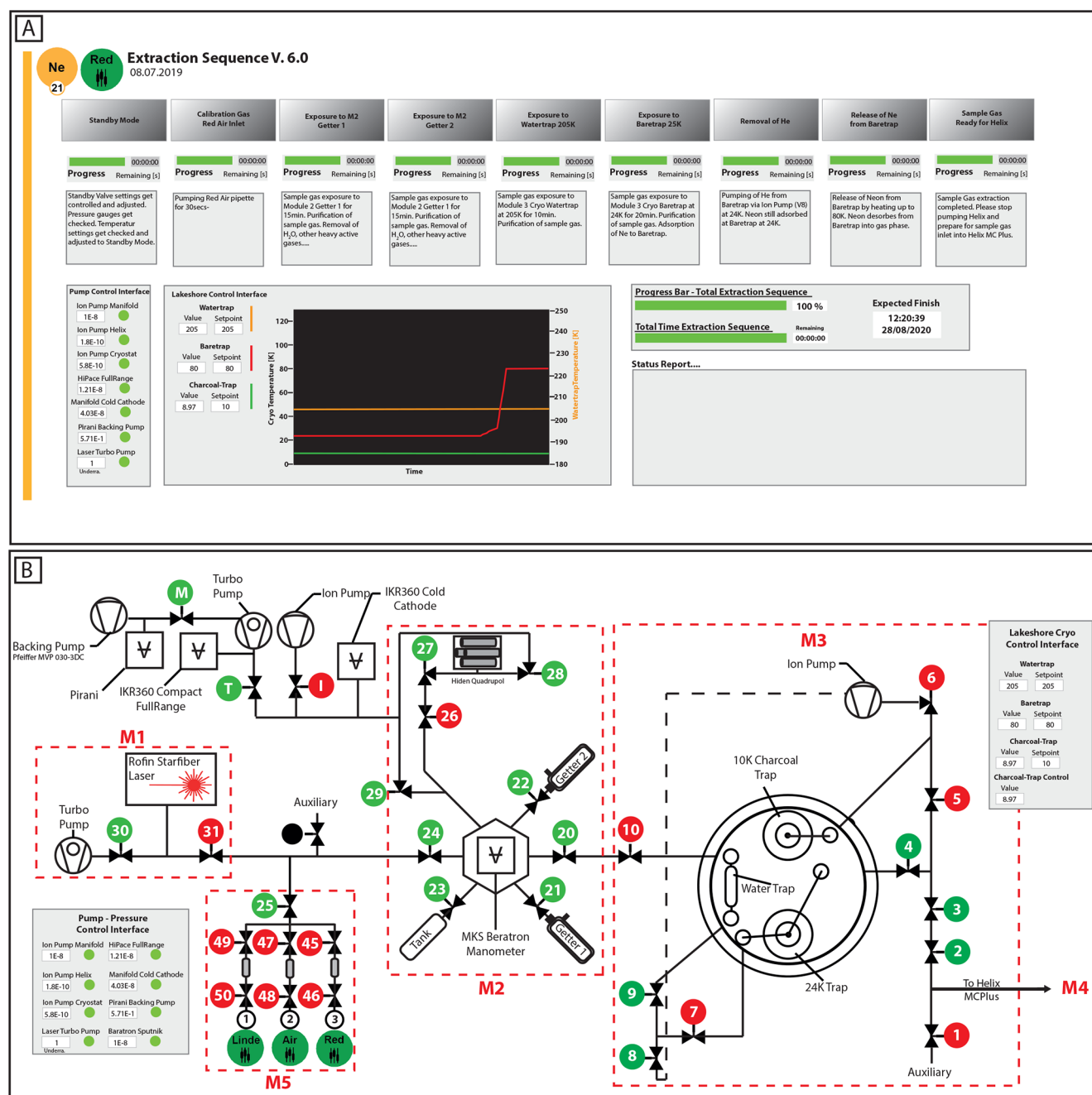
Figure 3. Screenshots of the operating VI program interface of the Cologne (CGN) Noble Gas Helix MC Plus. **(a)** The neon VI informs the user in real time about current data, such as pressure and temperature, as well as about the current status of the preparation. **(b)** Valve circuit overview. M1–M5 indicate the different modules of the extraction line. Valve numbers (1–10, 20–31, M, T, I) are coloured depending on the current state (green = open, red = closed).

nication. The main devices such as SAES getter control, Lakeshore Cryo-Controller, turbopumps and ion pumps already offered LabView-compatible Sub-VIs (Virtual Instrument, program codes), which were implemented into the operation VI (Fig. 3). The Agilent Ion Pump Control connection via the computer interfaces was written and developed in-house.

The gauges and controllers of the turbo pumps (Pfeiffer) and ion pumps (Agilent) are monitored via the operation VI (Fig. 3). Automatic safety protocols are implemented to protect the extraction line and equipment against sudden pressure increases. Temperature setting and monitoring of the three cold traps (Janis Cryostat) is performed by the
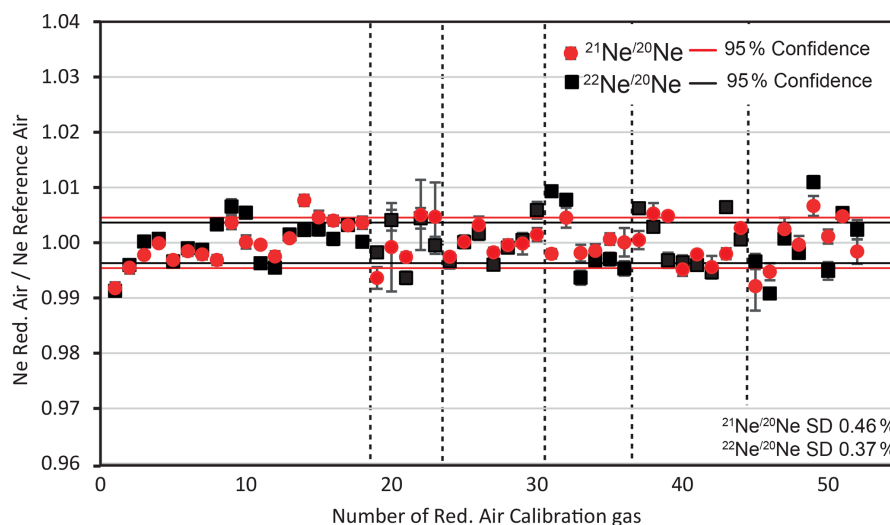
Figure 4. Reproducibility of standard gas RedAir measurements for sample runs at CGN noble gas lab, during the period between March 2020 and December 2020. Isotopic ratios are normalised to air for each run (mean of isotope ratios obtained in the run). The larger errors of the ^{21}Ne $/$ ^{20}Ne ratios of the second run may be due to the fact that prior to that run a longer development period of other noble gas species, and other sample materials, was conducted. During developmental work on a noble gas line, particularly when other gas species are analysed, the residual gas composition in the extraction line and in the mass spectrometer may change. The latter may affect the response and stability of multipliers (^{21}Ne is the only isotope we measure on the multipliers; thus it is the ^{21}Ne $/$ ^{20}Ne that shows the higher variability). Stippled black lines delineate individual runs. Error bars on individual data points are $\pm 1\sigma$. Symbol size is commonly larger than the corresponding error bars, which may therefore be hidden.

Lakeshore 336 controller, which in turn is controlled via the operation VI (Fig. 3).

LabView computing of the extraction sequence/protocol was programmed in single commands and steps, joined into command sequences connected in series as sub-VIs for each extraction protocol (various noble gases and sources of samples or calibration gas). Pressure and temperature control sequences are programmed in a continuous loop to ensure stability and safety during operation. For handling, a structured user–program interface was designed (Fig. 3), which provides the user with information about all parameters and total duration and additionally logs every extraction step.

3 Analytical procedure

Quartz samples are cleaned using standard procedures using dilute HF as etchant (Kohl and Nishiizumi, 1992). Up to 600 mg of quartz are loaded into tungsten cups and covered with a tungsten lid; the latter has a small hole to facilitate gas release. When opening the laser furnace for re-loading, the furnace is vented and purged with a continuous flow of pure nitrogen. In normal operation, after the initial installation and bake-out, the internal parts of the furnace are never again exposed to air. The tungsten cups and lids remain in the nitrogen atmosphere during sample (re-)loading. Cups are emptied with a suction micropicker (Micropicker MPC100, VU Amsterdam) while seated in the revolver, and weighed samples are transferred from the glass vials into
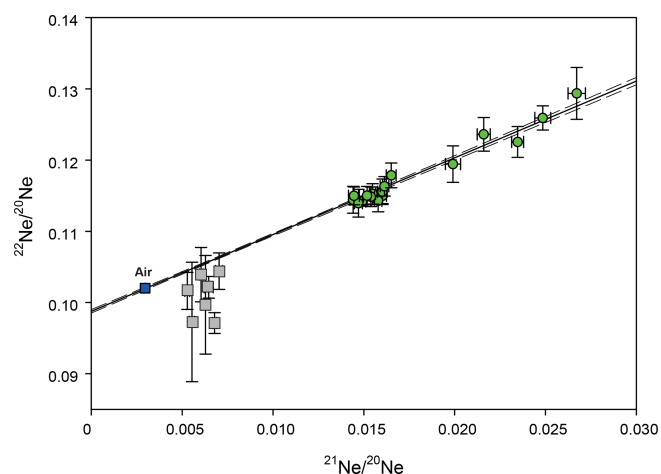

Figure 5. Neon three-isotope plot for CREU-1 intercomparison material measured in Cologne. Error bars are $\pm 1\sigma$. The cloud of green symbols displays single-step CREU extractions (100 W–15 min), the green dots to the right of the cluster are the initial heating (first extraction of a sample) steps of stepwise extractions (at varying laser output), grey rectangles are the subsequent steps that invariably had low abundance; for details see Table 1. Data of samples depicted in green are included in the regression calculation; data of the grey rectangles are excluded. The slope of the regression of the data (forced through air) is 1.078 ± 0.022 ($\pm 2\sigma$), which is indistinguishable from the published value of 1.108 ± 0.014 ($\pm 2\sigma$; Vermeesch et al., 2015). The dotted line denotes the 95 % confidence interval.
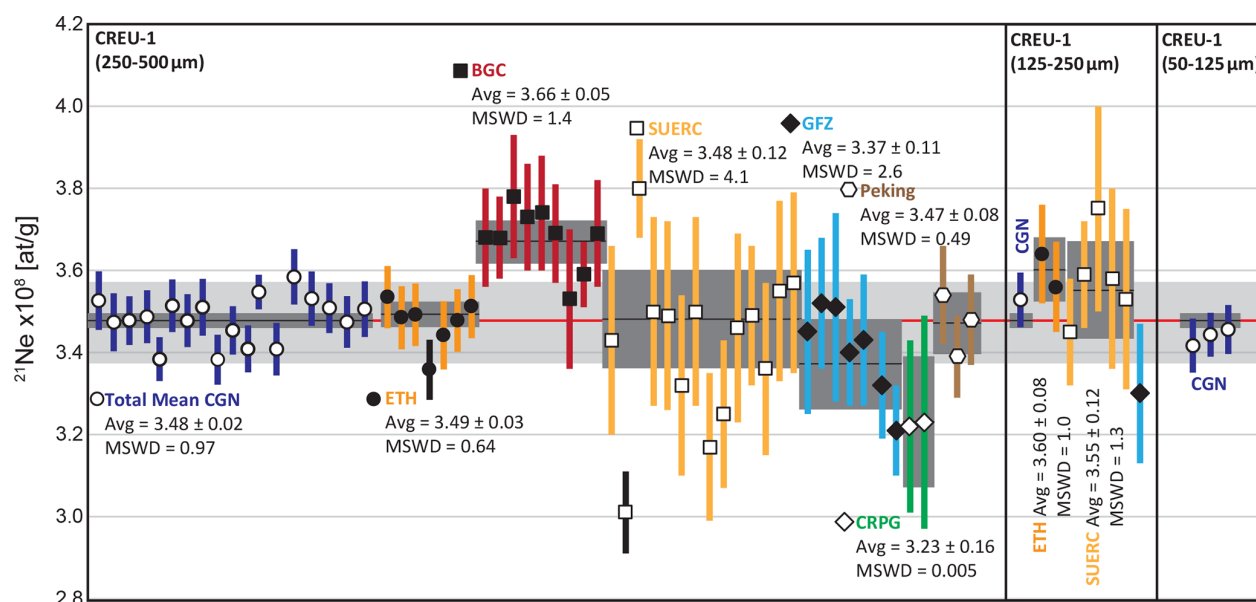
Figure 6. Compilation of CREU-1 ^{21}Ne concentrations ($\pm 2\sigma$ uncertainties) measured at Cologne (CGN), compared to reported ^{21}Ne concentrations from interlaboratory comparison from Vermeesch et al. (2015) and data from the Peking noble gas lab from Ma et al. (2015). Black bars were considered outliers by the original authors and not used for calculation of averages (Vermeesch et al., 2015). The data are divided into three sections, each for a different CREU-1 grain size analysed. The average ^{21}Ne concentration for CREU-1 of $3.48 \pm 10 \times 10^8$ atoms g^{-1} reported by Vermeesch et al. (2015) is marked as a light-grey band and a red line for the mean. Lab-individual error-weighted means are displayed as black lines with their respective uncertainty in dark grey. The average obtained for CREU-1 at Cologne (all grain sizes, $n = 22$) is $3.48 \pm 0.02 \times 10^8$ atoms g^{-1} ($\pm 2\sigma$; error-weighted standard deviation). The MSWD values (mean square of the weighted deviates ("reduced Chi-square", Mcintyre et al., 1966)) are reported for all individual laboratory means (Vermeesch et al., 2015; this study). CGN = University of Cologne, ETH = Eidgenössische Technische Hochschule Zürich, BGC = Berkeley Geochronology Center, SUERC = Scottish Universities Environmental Research Centre Glasgow, CRPG = Centre de Recherches Pétrographiques et Géochimiques Nancy, GFZ = Deutsches GeoForschungsZentrum Potsdam.

the cup through a miniature metal funnel (glass funnels produced undesirable static effects). After reloading, the sample revolver is heated by firing the laser on an empty cup; pressure $< 5 \times 10^{-9}$ mbar is usually achieved after pumping overnight. During this clean-up, and during subsequent analyses, the temperature of adjacent cups does not exceed 156.6 °C (verified with Indium wire). Cosmogenic Ne is extracted from quartz by heating the sample with a defocussed laser beam at 100 W for 15 min; at these settings, the cup insides reach ∼ 1200 °C. This temperature allows reliable extraction of cosmogenic neon (Vermeesch et al., 2015). After heating the furnace, it is allowed to cool for 5 min before the sample is expanded to the clean-up module.

For calibrations, the calibration gas is expanded for 30 s into the pipette, and the pipette volume is then expanded into the clean-up volume (Fig. 1). After this step, purification is identical for sample and calibration gases. The pipetting of calibration gas and the purification of sample and calibration gases are fully automatised.

Reactive gases are removed by sequential exposure to two metal getters (SAES NP50, Fig. 1); the first is operated hot, the other at room temperature. The gas is exposed to each for 15 min. Subsequently the gas is exposed to the water trap at

205 K for 10 min. The remaining inert gases are exposed to the bare-metal trap at 24 K for 20 min, which is then pumped for 5 min to remove helium from the sample gas (Fig. 1). The trap is then isolated and heated to 80 K, followed by 5 min holding time for re-equilibration. Neon is quantitatively released, and argon is quantitatively retained on the trap. Subsequently, Ne gas is expanded into the Helix MCMS for analysis. The bare trap at 80 K remains connected to the mass spectrometer during analysis, for pumping of CO_2 and Ar evolving from the mass spectrometer.

The configuration of the Helix is described above. For maximum sensitivity and precision for abundance determination (Wielandt and Storey, 2019), we use the widest (0.25 mm) source slit for neon analysis. We run the source at an electron energy of 115 eV, trap current of 200 µA and an acceleration voltage of 9.9 kV.

^{20}Ne is measured on the high-resolution L1 Faraday cup (fitted with 10^{13} Ω pre-amplifier), fully resolved from ^{40}Ar^{2+} and from molecular interferences such as HF$^+$, H$_2^{18}$O$^+$. ^{21}Ne is measured off-centre on the high-resolution L1 multiplier, at a position that is free from interference from ^{20}NeH$^+$. ^{22}Ne is measured at peak centre on the H1 Faraday cup (fitted with 10^{13} Ω pre-amplifier); interference from CO$_2^{2+}$ is

Table 1. CREU data.

Sample ID (g)	Mass power (W)	Extraction	^{20}Ne (10^9 atoms g^{-1})	^{21}Ne / ^{20}Ne	^{22}Ne / ^{20}Ne	^{21}Ne × cos. (10^6 atoms g^{-1})
01_CREU1 250–500 µm	0.0997	100	30.97 ± 0.15	0.01434 ± 0.00014	0.11381 ± 0.00129	352.7 ± 3.6
02_CREU1 250–500 µm	0.0993	100	29.81 ± 0.24	0.01461 ± 0.00015	0.11415 ± 0.00129	347.4 ± 3.5
03_CREU1 50–125 µm	0.1038	100	24.89 ± 0.15	0.01669 ± 0.00012	0.11646 ± 0.00170	341.7 ± 3.3
04_CREU1 50–125 µm	0.1319	100	25.73 ± 0.20	0.01634 ± 0.00018	0.11727 ± 0.00089	344.4 ± 2.7
05_CREU1 50–125 µm	0.1179	100	24.86 ± 0.17	0.01686 ± 0.00017	0.11614 ± 0.00130	345.6 ± 3.0
06_CREU1 125–250 µm	0.1078	100	27.00 ± 0.35	0.01603 ± 0.00022	0.11499 ± 0.00110	352.9 ± 3.3
07_CREU1 250–500 µm	0.1210	100	29.13 ± 0.36	0.01490 ± 0.00021	0.11417 ± 0.00065	347.8 ± 3.0
08_CREU1 250–500 µm	0.1105	100	30.46 ± 0.25	0.01441 ± 0.00018	0.11443 ± 0.00189	348.7 ± 3.2
09_CREU1 250–500 µm	0.1312	100	26.37 ± 0.32	0.01579 ± 0.00021	0.11428 ± 0.00153	338.4 ± 2.7
10_CREU1 250–500 µm	0.1128	100	29.92 ± 0.40	0.01470 ± 0.00022	0.11395 ± 0.00195	351.4 ± 3.2
11_CREU1 250–500 µm	0.1113	100	26.60 ± 0.33	0.01603 ± 0.00026	0.11556 ± 0.00179	347.8 ± 3.2
12_CREU1 250–500 µm	0.1053	100	30.56 ± 0.36	0.01445 ± 0.00030	0.11498 ± 0.00125	351.1 ± 3.5
13_CREU1 250–500 µm	0.1125	100	27.01 ± 0.24	0.01548 ± 0.00017	0.11526 ± 0.00143	338.3 ± 3.0
14_CREU1 250–500 µm	0.1210	100	26.21 ± 0.30	0.01614 ± 0.00024	0.11632 ± 0.00137	345.4 ± 3.0
15_CREU1 250–500 µm	0.1252	100	25.16 ± 0.19	0.01651 ± 0.00027	0.11786 ± 0.00174	340.9 ± 2.9
16_CREU1 250–500 µm	0.2063	100	28.54 ± 0.33	0.01539 ± 0.00020	0.11485 ± 0.00137	354.8 ± 2.1
17_CREU1 250–500 µm	0.1077	100	27.90 ± 0.30	0.01518 ± 0.00019	0.11502 ± 0.00129	340.9 ± 3.2
18_CREU1 250–500 µm	0.1126	30	16.44 ± 0.16	0.02160 ± 0.00036	0.12362 ± 0.00236	
	0.1126	50	8.61 ± 0.08	0.00628 ± 0.00019	0.09968 ± 0.00692	
	0.1126	70	5.71 ± 0.05	0.00528 ± 0.00013	0.10162 ± 0.00260	
	0.1126	100	3.92 ± 0.05	0.00554 ± 0.00015	0.09727 ± 0.00838	358.5 ± 3.4
19_CREU1 250–500 µm	0.1111	24	11.96 ± 0.17	0.02672 ± 0.00048	0.12936 ± 0.00364	
	0.1111	100	18.06 ± 0.23	0.00678 ± 0.00012	0.09711 ± 0.00146	353.2 ± 3.3
20_CREU1 250–500 µm	0.1301	24	14.27 ± 0.12	0.02347 ± 0.00033	0.12255 ± 0.00217	
	0.1301	100	16.51 ± 0.18	0.00646 ± 0.00025	0.10213 ± 0.00152	350.9 ± 3.0
21_CREU1 250–500 µm	0.1180	30	13.11 ± 0.15	0.02485 ± 0.00044	0.12592 ± 0.00170	
	0.1180	100	14.79 ± 0.09	0.00703 ± 0.00020	0.10440 ± 0.00256	347.5 ± 3.2
22_CREU1 250–500 µm	0.1075	50	18.42 ± 0.12	0.01991 ± 0.00042	0.11944 ± 0.00256	
	0.1075	100	12.35 ± 0.11	0.00604 ± 0.00010	0.10391 ± 0.00381	350.6 ± 3.4

corrected via monitoring of the ratio of double- to single-charged CO_2 in between samples and measurement of CO_2 during sample analysis, which we found to be stable at 0.0437 ± 0.001 for our system throughout the period for which the data we report here were obtained. The corresponding corrections of ^{22}Ne intensities are $< 0.3\%$ for one shot of RedAir calibration gas (~ 17 fmol ^{22}Ne). The uncertainties of the correction are $\sim 2\%$, which add $< 0.006\%$ uncertainty to the intensity determinations for RedAir. These values scale linearly for smaller or larger amounts of ^{22}Ne as found in samples. CO_2^+ is measured on the Faraday cup

of the Axial collector (fitted with 10^{13} Ω pre-amplifier). We refrain from analysing the larger neon beams (^{22}Ne, ^{20}Ne) on the multipliers, since we found that they are a significant source of CO_2 upon being hit by beams larger than those typical for ^{21}Ne signals (for analysing blanks, however, we use a multiplier for ^{20}Ne and ^{22}Ne). Besides, the Faraday cups have a superior linearity and stability over time (Wielandt and Storey, 2019). The mass spectrometer sensitivity, mass discrimination and multiplier vs. Faraday gain are calibrated with RedAir, which is measured at least once a day during sample runs. Each batch of samples includes at least one

measurement of ~ 100 mg CREU-1 (Vermeesch et al., 2015) to monitor the performance of the extraction and purification system. We are in the process of producing a new intercomparison material to replace CREU-1, whose supplies are limited and eventually will run too low for regular use.

4 Performance

The within-run reproducibility of neon isotope ratios as determined for calibration gas (RedAir, ~ 17 fmol atmospheric Ne) is similar for ^{21}Ne / ^{20}Ne and ^{22}Ne / ^{20}Ne ratios, with 0.46 % and 0.37 % ($\pm 1\sigma$, $n = 52$), respectively. This dispersion is larger than the uncertainty of individual measurements (Fig. 4); this feature, and the values for dispersion, are similar to those reported for other Helix Plus instruments (Honda et al., 2015; Wielandt and Storey, 2019). The second measurement period, with the increased uncertainties of the ^{21}Ne / ^{20}Ne ratios, was performed after an extended period of development work for other noble gas isotopes. We use the means and the uncertainty of the means of calibrations within runs to calibrate the measurement samples, i.e. propagate the observed dispersion in calculations of the abundance of cosmogenic ^{21}Ne in samples. Derived ^{21}Ne / ^{20}Ne and ^{22}Ne / ^{20}Ne ratios of 22 aliquots of CREU-1, including five power step extractions (Table 1), reveal a spallation line of 1.078 ± 0.022 ($\pm 2\sigma$), which is indistinguishable from the published value of 1.108 ± 0.014 ($\pm 2\sigma$; Vermeesch et al., 2015, Fig. 5). The calculated cosmogenic ^{21}Ne abundances from 22 aliquots of CREU-1 (Table 1) all agree within 2σ with their arithmetic mean ($348 \pm 10 \times 10^6$ atoms g^{-1}; $\pm 2\sigma$); thus, we may calculate an error-weighted mean: $348 \pm 2 \times 10^6$ atoms g^{-1} ($\pm 2\sigma$), which is indistinguishable from the published value ($348 \pm 10 \times 10^6$ atoms g^{-1}; Vermeesch et al., 2015; see Fig. 6). We conclude that the reproducibility and accuracy of the current set-up at the University of Cologne for determining cosmogenic ^{21}Ne in quartz is similar to or better than those reported for other laboratories worldwide (Vermeesch et al., 2015, Fig. 6; Farley et al., 2020; Ma et al., 2015).

5 Conclusion

The performance of the set-up for neon isotope measurements in the new noble gas laboratory at the University Cologne permits state-of-the art analysis of cosmogenic neon. We now regularly perform analysis of samples for cosmogenic neon for our running projects and are open to new scientific collaborations.

References

Binnie, S., Reicherter, K., Victor, P., González, G., Binnie, A., Niemann, K., Stuart, F., Lenting, C., Heinze, S., Freeman, S., and Dunai, T. J.: The origins and implications of paleochannels in hyperarid, tectonically active regions: The northern Atacama Desert, Chile, Global Planet. Change, 185, 103083, https://doi.org/10.1016/j.gloplacha.2019.103083, 2020.

Dunai, T. J.: Cosmogenic Nuclides: Principles, concepts and applications in the Earth surface sciences, Cambridge University Press, https://doi.org/10.1017/CBO9780511804519, 2010.

Dunai, T. J., Lopez, G. A. G., and Juez-Larre, J.: Oligocene-Miocene age of aridity in the Atacama Desert revealed by exposure dating of erosion-sensitive landforms, Geology, 33, 321–324, https://doi.org/10.1130/g21184.1, 2005.

Eberhardt, P., Eugster, O., and Marti, K.: A redetermination of the isotopic composition of atmospheric neon, Z. Naturforsch., 20a, 623–624, https://doi.org/10.1515/zna-1965-0420, 1965.

Espanon, V. R., Honda, M., and Chivas, A. R.: Cosmogenic ^{3}He and ^{21}Ne surface exposure dating of young basalts from Southern Mendoza, Argentina, Quat. Geochronol., 19, 76–86, https://doi.org/10.1016/j.quageo.2013.09.002, 2014.

Farley, K., Treffkorn, J., and Hamilton, D.: Isobar-free neon isotope measurements of flux-fused potential reference minerals on a Helix-MC-Plus10K mass spectrometer, Chem. Geol., 537, 119487, https://doi.org/10.1016/j.chemgeo.2020.119487, 2020.

Gillen, D., Honda, M., Chivas, A. R., Yatsevich, I., Patterson, D. B., and Carr, P. F.: Cosmogenic ^{21}Ne exposure dating of young basaltic lava flows from the Newer Volcanic Province, western Victoria, Australia, Quat. Geochronol., 5, 1–9, https://doi.org/10.1016/j.quageo.2009.08.004, 2010.

Györe, D., Tait, A., Hamilton, D., and Stuart, F. M.: The formation of NeH+ in static vacuum mass spectrometers and re-determination of ^{21}Ne / ^{20}Ne of air, Geochim. Cosmochim. Ac., 263, 1–12, https://doi.org/10.1016/j.gca.2019.07.059, 2019.

Honda, M., Zhang, X., Phillips, D., Hamilton, D., Deerberg, M., and Schwieters, J. B.: Redetermination of the ^{21}Ne relative abundance of the atmosphere, using a high resolution, multi-collector noble gas mass spectrometer (HELIX-MC Plus), Int. J. Mass Spectrom., 387, 1–7, https://doi.org/10.1016/j.ijms.2015.05.012, 2015.

Kohl, C. and Nishiizumi, K.: Chemical isolation of quartz for measurement of in-situ-produced cosmogenic nuclides, Geochim. Cosmochim. Ac., 56, 3583–3587, https://doi.org/10.1016/0016-7037(92)90401-4, 1992.

Ma, Y., Wu, Y., Li, D., and Zheng, D.: Analytical procedure of neon measurements on GV 5400 noble gas mass spectrometer and its evaluation by quartz standard CREU-1, Int. J. Mass Spectrom., 380, 26–33, https://doi.org/10.1016/j.ijms.2015.03.004, 2015.

Ma, Y., Wu, Y., Li, D., Zheng, D., Zheng, W., Zhang, H., Pang, J., and Wang, Y.: Erosion rate in the Shapotou area, northwestern China, constrained by in situ-produced cosmogenic ^{21}Ne in long-exposed erosional surfaces, Quat. Geochronol., 31, 3–11, https://doi.org/10.1016/j.quageo.2015.10.001, 2016.

McIntyre, G., Brooks, C., Compston, W., and Turek, A.: The statistical assessment of Rb-Sr isochrons, J. Geophys. Res., 71, 5459–5468, https://doi.org/10.1029/JZ071i022p05459, 1966.

McPhillips, D., Hoke, G. D., Liu-Zeng, J., Bierman, P. R., Rood, D. H., and Niedermann, S.: Dating the incision of the Yangtze River gorge at the First Bend using three-nuclide burial ages, Geophys. Res. Lett., 43, 101–110, https://doi.org/10.1002/2015GL066780, 2016.

Niedermann, S.: Cosmic-ray-produced noble gases in terrestrial rocks: dating tools for surface processes, Rev. Mineral. Geochem., 47, 731–784, 2002.

Niedermann, S., Graf, T., Kim, J., Kohl, C., Marti, K., and Nishiizumi, K.: Cosmic-ray-produced 21 Ne in terrestrial quartz: the neon inventory of Sierra Nevada quartz separates, Earth Planet. Sc. Lett., 125, 341–355, https://doi.org/10.1016/0012-821X(94)90225-9, 1994.

Ritter, B., Stuart, F. M., Binnie, S. A., Gerdes, A., Wennrich, V., and Dunai, T. J.: Neogene fluvial landscape evolution in the hyperarid core of the Atacama Desert, Sci. Rep., 8, 13952, https://doi.org/10.1038/s41598-018-32339-9, 2018.

Saxton, J.: The ^{21}Ne / ^{20}Ne ratio of atmospheric neon, J. Anal. Atom. Spectrom., 35, 943–952, https://doi.org/10.1039/D0JA00031K 2020.

Vermeesch, P., Balco, G., Blard, P. H., Dunai, T. J., Kober, F., Niedermann, S., Shuster, D. L., Strasky, S., Stuart, F. M., Wieler, R., and Zimmermann, L.: Interlaboratory comparison of cosmogenic Ne-21 in quartz, Quat. Geochronol., 26, 20–28, https://doi.org/10.1016/j.quageo.2012.11.009, 2015.

Wielandt, D. and Storey, M.: A new high precision determination of the atmospheric ^{21}Ne abundance, J. Anal. Atom. Spectrom., 34, 535–549, https://doi.org/10.1039/C8JA00336J, 2019.